

## A Very Narrow Spectral Band

Edward N. Lorenz<sup>1,2</sup>

*Received January 10, 1984*

---

The power spectrum of the variable  $z$  in the Lorenz equations with  $\sigma = 10$ ,  $b = 8/3$ , and  $r = 200$  appeared in previous work to contain a line superposed on a continuum. Analysis of an extended solution into consecutive segments with rather similar initial states, each segment spanning at least seven maxima of  $z$ , shows that the apparent line is actually a narrow band. Solutions spanning at least 14 000 maxima of  $z$  would be needed to resolve the band by standard computation procedures. Multiplication of the right side of each equation by the same function can convert the band to a line, while leaving the points of the attractor unchanged. It is proposed that the spectrum of a completely coupled autonomous flow is, in a certain sense, unlikely to contain a superposition of lines and a continuum.

---

**KEY WORDS:** Dynamical systems; chaos; power-spectrum analysis.

### 1. INTRODUCTION

One feature which distinguishes a chaotic autonomous flow or mapping from a periodic one is the nature of the power spectrum. A purely chaotic system, where almost every solution is uncorrelated with any sine curve, possesses a continuous spectral density function. A purely periodic system, where almost every solution is the sum of a finite or countable number of sine curves, possesses a set of spectral lines.

A mapping may also possess a mixed spectrum, where lines and a continuum are superposed; the lines may be treated as delta functions. Examples are the quadratic mapping

$$x_{n+1} = x_n^2 - a \quad (1)$$

---

<sup>1</sup> National Center for Atmospheric Research, Boulder, Colorado 80307.

<sup>2</sup> Permanent address: Department of Earth, Atmospheric, and Planetary Sciences, Massachusetts Institute of Technology, Cambridge, Massachusetts 02139.

where, for  $a = 1.5$ ,  $x_n$  alternates between high and low values, and the Hénon mapping,<sup>(1)</sup>

$$x_{n+1} = x_n^2 - a - bx_{n-1} \quad (2)$$

which, for  $a = 1.65$  and  $b = -0.1$ , exhibits similar behavior. For either system the subsequences with only even or only odd indices appear to be purely chaotic. More generally an attractor may contain several disjoint regions, and the successive points of a solution may occupy these regions in a fixed cyclic order. We have called such a mapping *semiperiodic*.

For a flow, the mapping defined by the states at successive occurrences of some key event may be semiperiodic. An example is the succession of local maxima  $Z_n$  of  $z$  in the Lorenz equations

$$\begin{aligned} \dot{x} &= -\sigma x + \sigma y \\ \dot{y} &= -xz + rx - y \\ \dot{z} &= xy - bz \end{aligned} \quad (3)$$

the dots denoting differentiation with respect to time  $t$ , where, for  $\sigma = 10$ ,  $b = 8/3$ , and  $r = 205$ ,  $Z_n$  alternates between high and low values,<sup>(2)</sup> and behaves much like  $x_n$  in Eq. (1) or (2). Semiperiodicity in such a mapping does not assure us of lines in the spectrum of the original flow, since the key events may occur at irregularly spaced times.

An autonomous flow may possess a mixed spectrum if the variables are not completely coupled. If the time derivatives of a subset of the variables do not contain the remaining variables, the subset by itself defines a flow, which may vary periodically. The remaining variables by themselves then effectively define a periodically forced flow, which may exhibit chaotic behavior superposed upon forced periodic behavior. An example is the system

$$\begin{aligned} \dot{w} &= w - \omega x - w^3 - wx^2 \\ \dot{x} &= \omega w + x - w^2x - x^3 \\ \dot{y} &= \gamma w - \delta y + z - z^3 \\ \dot{z} &= y \end{aligned} \quad (4)$$

where, in almost all solutions,  $w$  and  $x$  approach  $\cos \omega t$  and  $\sin \omega t$  asymptotically. When transient effects have disappeared, the system reduces to

$$\ddot{z} + \delta \dot{z} - z + z^3 = \gamma \cos \omega t \quad (5)$$

which is a form of Duffing's equation, and which, for  $\delta = 0.06$ ,  $\gamma = 0.57$ , and  $\omega = 1.19$ , behaves chaotically.<sup>(3,4)</sup> In Eqs. (4) and more generally, the partial decoupling may easily be disguised by a transformation of the

dependent variables. Whether or not a completely coupled autonomous flow may possess a mixed spectrum is less obvious.

A common procedure for estimating the spectral density function  $F(\omega)$  of a variable  $z(t)$  consists of obtaining a number of samples of  $z(t)$ , computing their cosine and sine transforms  $g(\omega)$  and  $h(\omega)$ , and then averaging  $g^2(\omega) + h^2(\omega)$  over the samples. An acceptable definition, which the procedure attempts to approximate, is

$$F(\omega) = \lim_{\tau \rightarrow \infty} \frac{1}{\tau} \left\langle \left| \int_{t_0}^{t_0 + \tau} e^{i\omega t} z(t) dt \right|^2 \right\rangle \quad (6)$$

where the pointed brackets denote an expected value or ensemble average. A range of values of  $\omega$  where  $F$  is exceptionally large constitutes a spectral band. For a true spectral line, where the oscillations of  $z(t)$  remain permanently correlated with those of  $\cos \omega t$  or  $\sin \omega t$ , the expected magnitude of the integral in Eq. (6) will increase as  $\tau$  instead of  $\tau^{1/2}$ , and the limit in Eq. (6) will not be finite.

Although power-spectrum analysis has long been a standard procedure in the study of natural chaotic processes, its application to simple differential-equation systems such as Eqs. (3)–(5) has been more limited. Holmes<sup>(3)</sup> and Ueda<sup>(5)</sup> have studied spectra of Eq. (5), and Holmes has compared them with spectra of Eqs. (3). Farmer et al.<sup>(6)</sup> have compared spectra of Eqs. (3) with those of the Rössler equations,<sup>(7)</sup> and have noted a much stronger tendency for apparent lines in the latter. They have also presented arguments suggesting that these apparent lines are really very narrow bands. Farmer<sup>(8)</sup> has studied the parameter dependence of the spectrum near the culmination of a period-doubling bifurcation sequence.

Recently we found that the spectrum of the variable  $z$  in Eqs. (3), for  $\sigma = 10$ ,  $b = 8/3$ , and  $r = 200$ , appeared to contain a single line together with a continuum, while, for  $r = 205$ , the continuum was accompanied by three lines. Our findings were based on a set of numerical solutions each spanning 344 maxima of  $z$ . When these solutions yielded no evidence that the apparent lines were really bands, we generated one solution, for  $r = 205$ , spanning 11 008 maxima of  $z$ , and found that these maxima were never more than 120 degrees out of phase with the maxima of an optimally chosen sine curve. We concluded that if the apparent lines were really bands, a much more extended solution would be needed to reveal the fact.

The specific purpose of this paper is to demonstrate, without actually obtaining a more extended solution, that for  $r = 200$  the apparent line is indeed a band, and to estimate its width and the amount of computation which would be needed to resolve it by standard procedures. A more general purpose is to indicate that spectra of chaotic flows often possess

extremely narrow bands, and to examine the likelihood that a completely coupled autonomous chaotic flow will possess a true spectral line.

## 2. COMPUTATION

Most of our computing time has been spent in generating numerical solutions of Eqs. (3), on which our subsequent conclusions are based. To solve the equations we choose a time increment  $\delta t$  and, at the beginning of each time step, find the first four derivatives of each variable; this is especially simple because the nonlinearities are quadratic. We advance through each time step by evaluating truncated Taylor series in  $\delta t$ . To find values within time steps we replace  $\delta t$  by a fraction of  $\delta t$ .

For  $\sigma = 10$ ,  $b = 8/3$ , and  $r = 200$ , we tentatively choose  $\delta t = 0.01$ . Figs. 1 and 2 show the typical behavior of the system, as indicated by a particular solution. Figure 1 shows the simultaneous behavior of the three variables. Evidently  $z$  possesses unequivocally identifiable local maxima and minima, but neither their strengths nor their spacings are uniform. Extrema of  $x$  alternate in sign and occur just before maxima of  $z$ , while minor and then major extrema of  $y$  precede extrema of  $x$ . There is no indication of superposed higher frequencies.

In Fig. 2 the upper curve shows the value  $Z_n$  of successive maxima of  $z$ , occurring at times  $t_n$  [or  $t(n)$ ], while the middle curve shows the lengths  $\Delta t_n = t_n - t_{n-1}$  of the time intervals between maxima. The values of  $t_n$  show

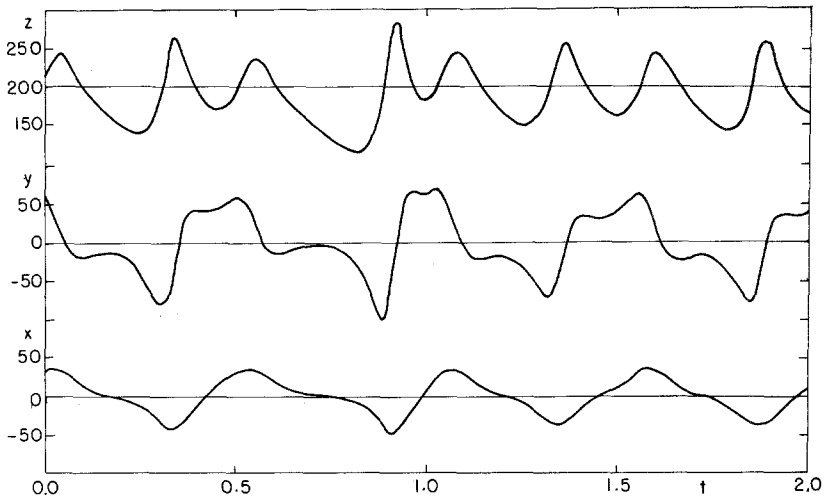


Fig. 1. Variations of  $z$  (upper curve),  $y$  (middle curve), and  $x$  (lower curve) in numerical solution of Eqs. (3), with  $\sigma = 10$ ,  $b = 8/3$ ,  $r = 200$ , and  $\delta t = 0.01$ .

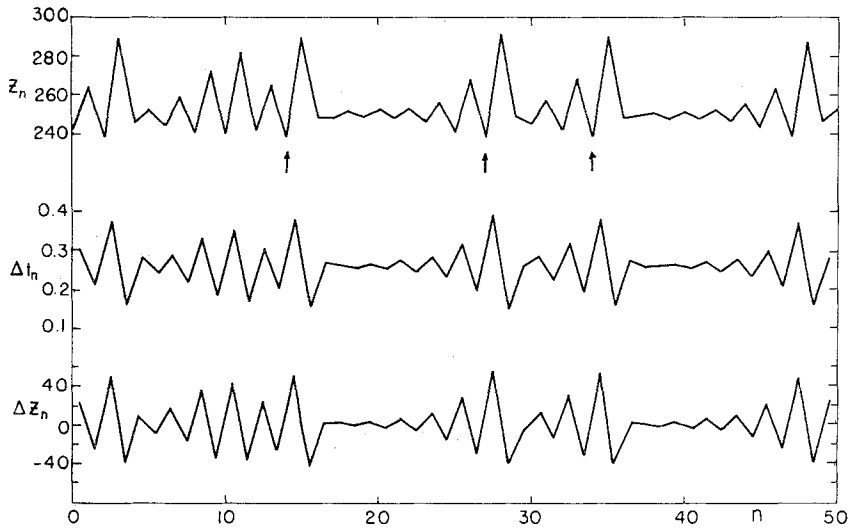


Fig. 2. Successive maxima  $Z_n$  of  $z$  (upper), time intervals  $t_n$  between maxima of  $z$  (middle), and successive changes  $\Delta Z_n$  in  $Z_n$  (lower), in same numerical solution as in Fig. 1.

considerable variation about their long-term average  $d$ , about 0.2592. The lower curve shows the successive changes  $\Delta Z_n = Z_n - Z_{n-1}$  in the strengths of the maxima. The middle and lower curves prove to be nearly indistinguishable.

If  $\Delta t_n$  and  $\Delta Z_n$  were perfectly correlated, the spectrum of  $z$  would possess a true line at  $\omega = 2\pi/d$ , since  $t_n$  would never completely lose phase with  $t_0 + nd$ . Actually the correlation is imperfect, but it is so high that the phase loss cannot grow rapidly. To determine whether it grows at all we follow another approach.

A feature of the attractor  $A$  of Eqs. (3) which is common to that of many chaotic flows is the presence of an infinite number of unstable periodic orbits  $Q_1, Q_2, \dots$  in  $A$ . An arbitrary point  $P$  in  $A$  moving along its orbit will, on an infinite number of separate occasions, pass arbitrarily close to any periodic orbit  $Q_j$ ; the closer a given approach, the longer the time before  $P$  recedes from  $Q_j$ . It follows that the oscillations of any variable must eventually lose any temporary agreement with those of any pure sine curve, unless the period of the sine curve is a divisor of the period  $2\pi/\omega_j$  of  $Q_j$ . Thus we cannot expect  $F(\omega)$  to have any true lines except at multiples of  $\omega_j$ , and, unless  $\omega_1, \omega_2, \dots$  have a common multiple, we cannot expect any lines at all.

A solution which is periodic in  $x, y$ , and  $z$  must also be periodic in  $Z_n$ . We shall call the number  $M$  of maxima of  $z$  before  $z$  repeats its behavior

the *order* of the solution, and call the solution an  $M$ -loop solution. We shall call time  $\Delta T$  required for  $z$  to repeat its behavior the *period*, and the ratio  $\Delta T/M$  the *subperiod*, even though  $x$  and  $y$  will have reversed their signs if  $M$  is odd.

Figure 2 suggests that 1-loop and 7-loop solutions may exist with initial conditions close to the conditions at  $t_{18}$  and  $t_{26}$ . Such solutions are readily found by successive approximation. The computed subperiods are respectively 0.258394 and 0.260104.

These values, although unequal, are so close that we must consider the possibility that their difference is an artifact of the numerical procedure. Accordingly, we have redetermined the subperiods, using shorter time steps. With  $\delta t = 0.005$  the subperiods are 0.258351 and 0.260013; with  $\delta t = 0.001$  they are 0.258349 and 0.260009. We conclude that the subperiods are definitely unequal, and that the periods cannot have a common divisor close to either subperiod. There is therefore no spectral line near  $\omega_0$ . Use of the longer time step  $\delta t = 0.01$  hardly alters the subperiods, but it changes their difference noticeably, and in the remaining computations we have let  $\delta t = 0.005$ .

Returning to Fig. 2, we note that  $Z_n$  tends to alternate between higher and lower values, but occasionally increases or decreases twice in a row, so that the phase of the alternations is reversed. These reversals occur shortly after exceptionally high values of  $Z_n$ , which occur immediately after exceptionally low values. We shall denote the times  $t(n_0), t(n_1), \dots$  of these low values by  $T_0, T_1, \dots$ , and call the segment of the solution of length  $D_k = T_k - T_{k-1} = t(n_k) - t(n_{k-1})$  extending from  $T_{k-1}$  to  $T_k$  a *reversing segment* of order  $m_k = n_k - n_{k-1}$ , or an  $m_k$ -loop segment. We shall call the ratio  $d_k = D_k/m_k$  the *sublength*. In Fig. 2 the times  $T_0 = t_{13}$ ,  $T_1 = t_{26}$ , and  $T_2 = t_{33}$  are indicated by arrows;  $T_0$  and  $T_1$  are the initial points of a 13-loop segment of sublength 0.25898 and a 7-loop segment of sublength 0.26012. No reversals follow the rather low maxima at  $t_2$  and  $t_{47}$ .

In Fig. 3 the upper curve shows successive values of  $m_k$ , plotted logarithmically, occurring in a new solution with  $\delta t = 0.005$ . Evidently 3-loop and 5-loop segments never occur, while about 20% of the segments are of order 7. The lower curve shows the corresponding values of  $d_k$ . The total range of  $d_k$  is remarkably small, in view of the large range of  $\Delta t_n$ . No sublengths are as short as the 1-loop subperiod (the bottom line in Fig. 3), while none are much longer than the 7-loop subperiod. In addition,  $d_k$  and  $\log m_k$  have a high negative correlation. Examination reveals that this correlation is due largely, but not entirely, to the values of  $d_k$  when  $m_k = 7$ ; these are all close to the 7-loop subperiod and are completely separated from the remaining values of  $d_k$ .

Extension of the solution to 338 segments containing 6764 maxima indicates no systematic arrangement of the successive values of  $m_k$ . Like-

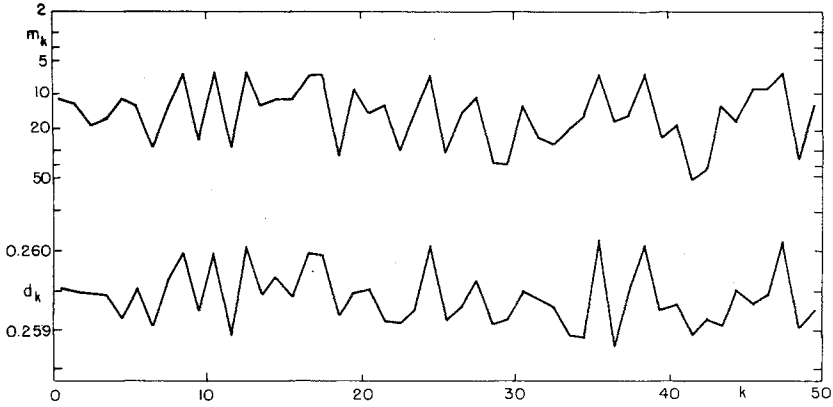


Fig. 3. Orders  $m_k$  of successive reversing segments (upper), and subperiods  $d_n$  of reversing segments (lower), in numerical solution of Eqs. (3) with  $\sigma = 10$ ,  $b = 8/3$ ,  $r = 200$ , and  $\delta t = 0.005$ .

wise the values of  $D_k - m_k d$ , which represent the successive shifts in phase difference between  $z(t)$  and a sine curve of optimally chosen period  $d = 0.259226$ , show a serial correlation of only  $-0.06$  at one lag. Thus the length and order of one segment appear to tell us very little about the lengths and orders of the following segments.

In summary,  $z(t)$  may be expressed as a succession of intervals of length  $\Delta t_n$  having a mean  $d = 0.2592$  and a range of  $0.2396$ , and the consecutive values of  $d_n$  will have a high negative correlation. Alternatively,  $z(t)$  may be expressed as a succession of segments of length  $D_k$  and order  $m_k$ , where  $m_k$  has a mean  $m = 20.0$ , while  $D_k$  has a mean  $D = md = 5.184$  and  $D_k - m_k d$  has a standard deviation  $\epsilon = 0.0055$ , and successive values of  $D_k - m_k d$  will occur in essentially random order. The latter formulation will allow us to estimate the width of the spectral band at  $\omega_0 = 2\pi/d$ .

With  $z(t)$  analyzed into segments, Eq. (6) becomes

$$F(\omega) = \lim_{K \rightarrow \infty} \frac{1}{T_K - T_0} \left\langle \left| \sum_{k=1}^K \int_{T_{k-1}}^{T_k} e^{i\omega t} z(t) dt \right|^2 \right\rangle \quad (7)$$

We note first that between  $T_{k-1}$  and  $T_k$  there is very little phase shift of the maxima of  $z(t)$  relative to those of  $\cos \omega t$ , provided that  $\omega$  is close to  $\omega_0$ . The values of the separate integrals in (7) thus depend mainly upon the lengths  $T_k - T_{k-1}$  and the accumulated phase shift up to time  $T_{k-1}$  or  $T_k$ . We therefore let

$$\int_{T_{k-1}}^{T_k} e^{i\omega t} z(t) dt = c_k m_k e^{i\omega T_k} \quad (8)$$

and assume that the relative variations of  $c_k$  are small compared to those of

$\cos \omega T_k$  or  $\sin \omega T_k$ , and may be neglected. Thus

$$F(\omega) = \lim_{K \rightarrow \infty} \frac{c^2}{T_K - T_0} \sum_{j,k=1}^K \langle m_j m_k e^{i\omega(T_k - T_j)} \rangle \quad (9)$$

We now assume that the width of the band would not be greatly altered if all segments possessed the same order  $m = 20$ , with the standard deviation of  $D_k$  still equal to  $\epsilon = 0.0055$ . Assuming that successive values of  $D_k$  are independent, so that the variance of  $T_k - T_j$  is  $|k - j|\epsilon^2$ , and approximating the distribution of  $D_k$  by a Gaussian distribution (actually it is skewed), we find that

$$F(\omega) = c^2 m^2 \sum_{j=-\infty}^{\infty} e^{ij\omega D} e^{-(1/2)j\omega^2 \epsilon^2} \quad (10)$$

Letting  $\omega = \omega_0 + \alpha$ , where  $\alpha/\omega_0$  is small, and noting that both the positive and negative terms in Eq. (10) form geometric series, we obtain

$$F(\omega_0 + \alpha) = c^2 m^2 \sinh\left(\frac{1}{2}\omega^2 \epsilon^2\right) / \left[ \cosh\left(\frac{1}{2}\omega^2 \epsilon^2\right) - \cos(\alpha D) \right] \quad (11)$$

Since  $\omega\epsilon$  is small, we find, for  $\alpha D$  small, that

$$F(\omega_0 + \alpha)/F(\omega_0) = \omega^4 \epsilon^4 / (\omega^4 \epsilon^4 + 4\alpha^2 D^2) \quad (12)$$

Thus, for example, if  $F(\omega_0 + \alpha)$  is to be one half as large as  $F(\omega_0)$ ,  $\alpha D = 1/2\omega_0^2 \epsilon^2$ , or  $\alpha/\omega_0 = \pi\epsilon^2/md^2$ .

With the appropriate numerical values,  $\alpha/\omega_0 = 7.1 \times 10^{-5}$ , or about  $1/14000$ . This means that if the expected spectrum, computed by standard procedures, is to show a peak value at one point with values half as large as the two adjacent points, the three points must be points 13999, 14000, and 14001, and the solutions whose Fourier transforms are evaluated must span 14000 maxima of  $z$ , or 700 segments. Higher resolution would require longer solutions, and, in any event, several solutions are needed for a representative average. The required computations would exceed that of the present study by at least an order of magnitude.

### 3. DISCUSSION

Our procedure may appear somewhat haphazard. We have taken it for granted that reversing segments may be unequivocally defined. Without invoking full mathematical rigor we can place our conclusions on a sounder basis.

Figure 4 is a plot of 1000 consecutive maxima  $Z_n$  of  $z$  against the immediately preceding maxima  $Z_{n-1}$ . The points appear to fall on a principal curve covering the full range of  $Z_n$ , and a shorter auxiliary curve



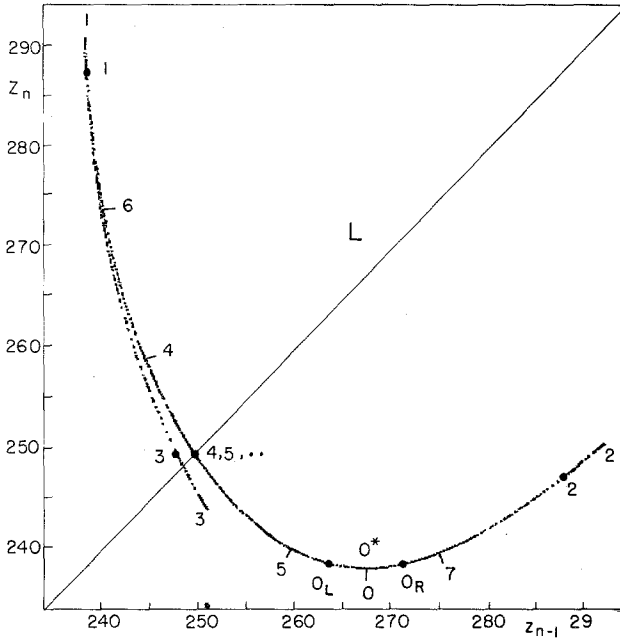


Fig. 4. Values of maxima  $Z_n$  of  $z$  versus values of previous maxima  $Z_{n-1}$ , in same numerical solution as in Fig. 3. Numbers 0, 1, ... opposite hatch marks or at ends of curves indicate points  $P_0^*, P_1^*, \dots$  referred to in text. Numbers  $0_L, 0_R, 1, \dots$  opposite large dots refer to points  $P_{0L}, P_{0R}, P_1^*, \dots$ . Diagonal line  $L$  is line  $Z_n = Z_{n-1}$ .

merging with it at the upper left. Points on the auxiliary curve follow points to the right of the rounded minimum, so that each point  $(Z_{n-1}, Z_n)$  determines  $(Z_n, Z_{n+1})$  unambiguously. The diagonal line  $L$ , where  $Z_n = Z_{n-1}$ , intersects the principal curve at the fixed point, which corresponds to the 1-loop solution. Points above or below  $L$  correspond to increases or decreases in  $Z$ .

If point  $P_0^*$  with coordinates  $(Z_{-1}^*, Z_0^*)$  is at the rounded minimum, point  $P_1^*$  with coordinates  $(Z_0^*, Z_1^*)$  is at the extreme upper left. The succeeding points  $P_2^*$  and  $P_3^*$  then are at the right end of the principal curve and the lower end of the auxiliary curve, and both lie below  $L$ , so that a reversing segment begins at  $Z_0^*$ . Points  $P_4^*$  to  $P_7^*$  lie on alternate sides of  $L$ , and  $P_5^*$  and  $P_7^*$  straddle  $P_0^*$ .

If  $P_0'$  with coordinates  $(Z'_{-1}, Z_0')$  coincides with point  $P_{0L}$  or  $P_{0R}$  lying somewhat to the left or right of  $P_0^*$ , points  $P_1', P_2',$  and  $P_3'$  will lie, respectively, below  $P_1^*$ , to the left of  $P_2^*$ , and above  $P_3^*$ . If  $P_{0L}$  or  $P_{0R}$  is suitably chosen,  $P_4'$ , and hence  $P_5' \dots$ , will fall on the fixed point.

If  $P_0$  lies between  $P_{0L}$  and  $P_{0R}$ ,  $P_1$  will lie between  $P_1^*$  and  $P_1'$ , etc. Thus, if  $P_0$  is suitably chosen, either to the left or right of  $P_0^*$ ,  $P_7$  will coincide with  $P_0$ . There are therefore two 7-loop solutions, one with  $Z_0 < Z_0^*$  and one with  $Z_0 > Z_0^*$ . The solution whose subperiod we previously determined was the former. Estimates of the subperiod of the latter, with  $\delta t = 0.01, 0.005,$  and  $0.001,$  are  $0.260051, 0.259965,$  and  $0.259961.$

It is evident that two successive points  $P_n, P_{n+1}$  cannot lie on the same side of  $L$  unless  $P_n$  lies between  $P_3^*$  and  $P_3'$  and above  $L$ , or  $P_{n+1}$  lies between  $P_3^*$  and  $P_3'$ , and below  $L$ . In these cases  $P_{n-2}$ , or  $P_{n-1}$ , lies between  $P_{0L}$  and  $P_{0R}$ , while  $P_{n+1}$  and  $P_{n+3}$ , or  $P_{n+2}$  and  $P_{n+4}$ , lie to the left of  $P_{0L}$ . There can therefore be no 3-loop or 5-loop segments.

We can examine the correlation between  $\Delta t_n$  and  $\Delta Z_n$  in similar detail. Figure 5 shows 1000 consecutive values of  $\Delta t_n$  plotted against the corresponding values of  $\Delta Z_n$ . Here also the points appear to be confined to a principal curve and an auxiliary curve, and the correlation, although high, is clearly imperfect. If we rotate Fig. 4 counterclockwise through  $225^\circ$ , the

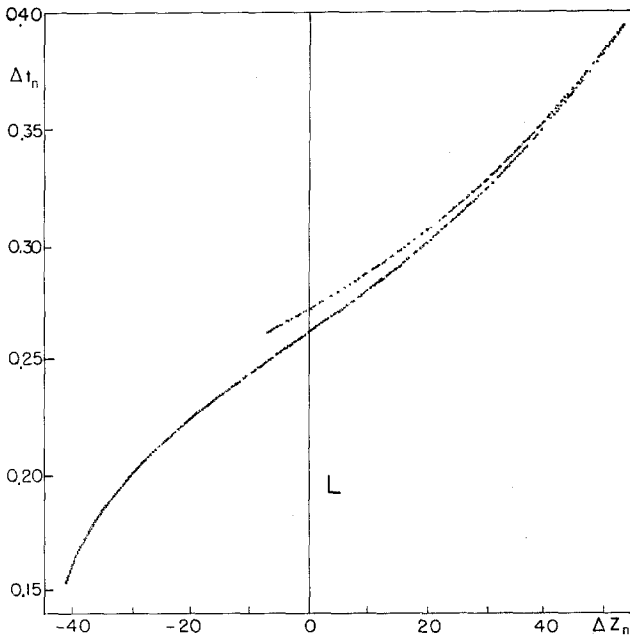


Fig. 5. Times intervals  $\Delta t_n$  between consecutive maxima of  $z$  versus differences  $\Delta Z_n$  between values of consecutive maxima, for same numerical solution as in Fig. 3. Vertical line  $L$  is line  $\Delta Z_n = 0$ .

new abscissa is  $\Delta Z_n$ , while  $L$  becomes the vertical line  $Z_n = 0$ , after which the figure may easily be distorted into Fig. 5.

The mapping from  $(Z_{n-1}, Z_n)$  to  $(Z_n, Z_{n+1})$  in Fig. 4 is actually a Poincaré mapping. Ordinarily in such a mapping, the values of two variables, say,  $x$  and  $y$ , at some key time, say when  $z$  crosses the surface  $z = z^*$  toward lower values, determine the values  $x', y'$ , of  $x$  and  $y$  at the following crossing. Here we have replaced the plane by the hyperboloid  $z = xy/b$ , and  $x$  and  $y$  by two functions of  $x$  and  $y$ , namely,  $xy/b$  and  $x'(x, y)y'(x, y)/b$ . The curves in Fig. 4 form the attractor of this mapping.

Just as points with equal ordinates on the two sides of  $P_0^*$  are followed by points with equal abscissas on the principal and auxiliary curves, so we would expect points on these curves with equal ordinates to be followed by points with equal abscissas and distinct ordinates, and hence on separate curves. Such curves may in fact be observed by redrawing Fig. 4 with sufficient magnification; a second auxiliary curve lies above the principal curve and terminates at  $P_4^*$ . Continuing with this reasoning, we conclude that the attractor should consist locally of a Cantor set of curves. Globally some of these curves are joined; the apparent ends at  $P_1^*, P_2^*, \dots$  are not ends nor even cusps, but are points of extremely large curvature.

The mapping closely resembles the Hénon mapping of Eq. (2), with a small negative  $b$  (a positive  $b$  would place the auxiliary curve to the right of the principal curve). We can illustrate the Cantor-set structure of the attractor schematically by displaying the actual Hénon attractor for a larger negative  $b$ , choosing  $a$  so that there are periodic solutions of order 7 but not order 5. Figure 6 shows 4000 points on the Hénon attractor for  $a = 2.238$  and  $b = -0.4$ . Two additional auxiliary curves, appearing to terminate at  $P_4^*$  and  $P_5^*$ , are resolved. Points  $P_4'$  and  $P_5'$  lie on these curves;  $P_6', P_7' \dots$  lie on curves which are still not distinguishable as separate curves, and appear as a single principal curve. Our conclusions concerning the impossibility of 3-loop and 5-loop segments are unchanged.

By analogy with Fig. 4, we should expect Fig. 5 to contain a Cantor set of curves. Evidently it does; with sufficient magnification the principal curve in Fig. 5 appears to be two curves.

We have noted<sup>(2)</sup> that for  $r > 203.4$  there are no periodic solutions of odd order  $> 1$ . By analogy with Eqs. (1) and (2) we should expect some intermediate values of  $r$  where one 7-loop solution is stable. We find such values extending from 200.65 to 200.67. Here the attractor reduces to 7 points, and the spectrum contains lines and no continuum.

For slightly higher values of  $r$ , 7-loop segments no longer occur, and the shortest segments are of order 9. The differences between the various sublengths are presumably smaller, and the spectral band at  $\omega_0$  is corre-

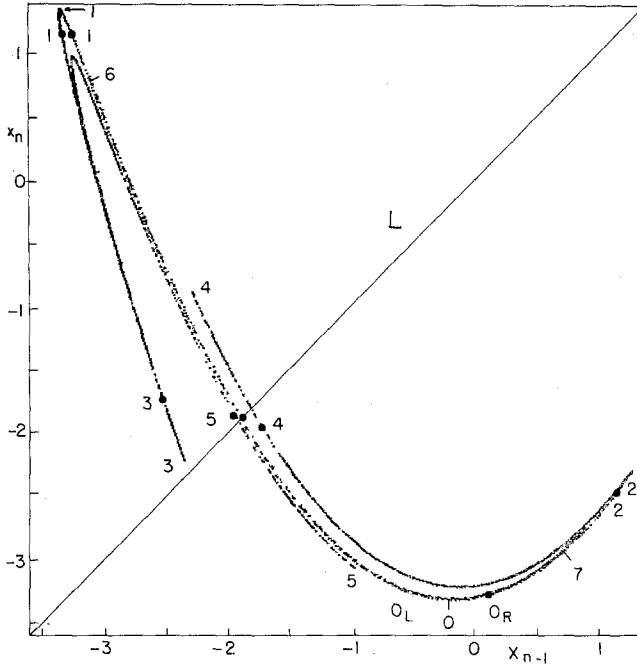


Fig. 6. Values of  $x_n$  versus values of  $x_{n-1}$  in Hénon mapping of Eqs. (2), for  $a = 2.238$  and  $b = -0.4$ . Numbers opposite hatch marks, at ends of curves, or opposite large dots have same meaning as in Fig. 4. Line  $L$  is line  $x_n = x_{n-1}$ .

spondingly narrower. For  $r = 205$  the reversing segments would have to be defined in terms of phase reversals in the sequence  $Z_0, Z_2, Z_4, \dots$ , and the spectral bands could be exceedingly narrow.

#### 4. CONCLUDING REMARKS

We have examined the power spectrum of one variable  $z$  in a dynamical system, which in an earlier study appeared to consist of a continuum and a line. We have determined that the apparent line is actually a band. Our most remarkable finding is the extreme narrowness of the band, compared to bands in the spectra of many natural chaotic phenomena, such as the sunspot cycle; this was not suggested to us by the many intensively investigated features of Eqs. (3) such as homoclinic explosions.<sup>(9)</sup> Solutions spanning more than 10000 maxima of  $z$  would be needed to establish by direct computation that the band is not a line.

We have derived a Poincaré mapping which expresses each maximum of  $z$  as a function of the previous two maxima. The Hénon mapping with a

small negative  $b$  serves as a convenient inexpensive approximation to the Poincaré mapping. What the Hénon mapping and the Poincaré mapping do not reveal is the time intervals between successive maxima of  $z$ . This becomes evident when we note that if the right-hand side of each equation is multiplied by the same differentiable scalar function  $f(x, y, z)$ , with positive upper and lower bounds, the Poincaré mapping, and in fact the points of the attractor  $A$ , will be left unaltered. At the same time, the time intervals  $\Delta Z_n$  between maxima of  $z$ , and the frequency with which different parts of  $A$  are visited, may be changed. It follows that the power spectrum may be changed.

Multiplication by  $f$  effectively replaces  $t$  by a new independent variable  $\theta$  where  $dt/d\theta = f$ . For Eqs. (3), a suitable choice of  $f$  can replace the spectral band by a line. If, for example,

$$\tan \theta = (xy - bz)/(\omega_0 z^* - \omega_0 z) \quad (13)$$

where  $z^*$  is a value, say,  $r - 1$ , which  $z$  invariably crosses between successive extrema,

$$f = [\omega_0^2(z^* - z)^2 + \dot{z}^2]/[\omega_0(z^* - z)\ddot{z} + \omega_0\dot{z}^2] \quad (14)$$

Numerical integration indicates that the denominator in Eq. (14) will never vanish in  $A$ , whence the maxima and minima of  $z$  will occur when  $\theta$  is a multiple of  $\pi$ , while  $z = z^*$  at odd multiples of  $\pi/2$ . Thus there will be a spectral line at period  $2\pi$ .

In equalizing the intervals between maxima we have also partially decoupled the variables. Equation (13) implies that

$$z = (xy \cos \theta - \omega_0 z^* \sin \theta)/(b \cos \theta - \omega_0 \sin \theta) \quad (15)$$

when this value is substituted, the new system reduces to a periodically forced system in  $x$  and  $y$ .

The original intervals between maxima vary considerably, so that  $f$ , as given by Eq. (14), must vary likewise. By contrast, the sublengths of the reversing segments vary only slightly. We wonder whether a function  $f$  of comparably slight variation can equalize the sublengths, without equalizing the individual intervals. We wonder also whether, in this event, the variables will become partially decoupled.

In summary, the spectral properties of a chaotic flow need not be the same as those of a Poincaré mapping derived from it. A superposed line in either spectrum does not imply such a line in the other spectrum. For some completely chaotic systems, including Eqs. (3), a simple transformation of the independent variable can produce a spectral line.

Mappings with mixed spectra are common; they occur, for example, just beyond the culmination of every period-doubling bifurcation se-

quence.<sup>(10,2)</sup> By contrast, autonomous flows with mixed spectra appear, in a certain sense, to be exceptional. Just as a multiplicative function may sometimes equalize the time intervals between key events, so one may sometimes render them unequal. Some function can convert the partially decoupled Eqs. (4), for example, into a completely coupled system, with no spectral line. Among all possible choices of positively bounded differentiable functions, those which will equalize a chosen set of intervals are, in a certain sense, much rarer than those which will make them unequal.

## ACKNOWLEDGMENTS

The National Center for Atmospheric Research, where most of this study was performed, is supported by the National Science Foundation. A portion of the work was performed at the author's permanent address, and was supported by the GARP Program of the Atmospheric Sciences Section, National Science Foundation, under Grant No. 82-14582 ATM.

## REFERENCES

1. M. Hénon, *Commun. Math. Phys.* **50**:69 (1976).
2. E. N. Lorenz, *Ann. N.Y. Acad. Sci.* **357**:282 (1980).
3. P. R. Holmes, *Appl. Math. Modelling* **1**:362 (1977).
4. J. Guckenheimer and P. R. Holmes, *Nonlinear Oscillations, Dynamical Systems, and Bifurcations of Vector Fields* (Springer, New York, 1983).
5. Y. Ueda, *J. Stat. Phys.* **20**:181 (1979).
6. J. D. Farmer, J. Crutchfield, H. Froehling, N. Packard, and R. Shaw, *Ann. N.Y. Acad. Sci.* **357**:453 (1980).
7. O. E. Rössler, *Phys. Lett. A* **57**:397 (1976).
8. J. D. Farmer, *Phys. Rev. Lett.* **47**:179 (1981).
9. C. Sparrow, *The Lorenz Equations: Bifurcations, Chaos, and Strange Attractors* (Springer, New York, 1982).
10. S. Grossmann and S. Thomae, *Z. Naturforsch.* **32a**:1353 (1977).